# Most of the Rhamnogalacturonan-I from Cultured Arabidopsis Cell Walls is Covalently Linked to Arabinogalactan-Protein

Li Tan<sup>1,2\*</sup>, Liang Zhang<sup>1,2,3</sup>, Ian Black<sup>1,2</sup>, John Glushka<sup>1</sup>, Breeanna Urbanowicz<sup>1,2,3</sup>, Christian Heiss<sup>1,2</sup>, Parastoo Azadi<sup>1,2</sup>

<sup>1</sup>Complex Carbohydrate Research Center, <sup>2</sup>DOE Center for Plant and Microbial Complex Carbohydrates, <sup>3</sup>Department of Biochemistry and Molecular Biology, University of Georgia, 315 Riverbend Road, Athens, GA 30602

\* Corresponding author. Tel: 1-706-542-4468, fax: 1-706-542-4412.

Email address: tan@ccrc.uga.edu

Abstract

To characterize a purified rhamnogalacturonan-I (RG-I) containing both RG-I and

arabinogalactan-protein (AGP) types of glycosyl residues, an AGP-specific β-1,3-

galactanase that can cleave the AG backbone and release the AG sidechain was applied to

this material. Carbohydrate analysis and NMR spectroscopy verified that the galactanase-

released carbohydrate consists of RG-I covalently attached to the AG sidechain, proving

a covalent linkage between RG-I and AGP. Size exclusion chromatography-multiangle

light scattering-refractive index detection revealed that the galactanase-released RG-I has

an average molecular weight of 41.6 kDa, which, together with the percentage of pectic

sugars suggests an RG-I-AGP comprising one AGP covalently linked to two RG-I

glycans. Carbohydrate analysis and NMR results of the RG-I-AGP, the galactanase-

released glycans, and the RG lyase-released glycans demonstrated that the attached RG-I

glycans are decorated with  $\alpha$ -1,5-arabinan,  $\beta$ -1,4-galactan, xylose, and 4-O-Me-xylose

sidechains. Our measurement suggests that the covalently linked RG-I-AGP is the major

component of the traditionally prepared RG-I.

**Keywords:** RG-I-AGPs, RG-I, AGPs, covalent linkage, RG-I size, NMR

## 1. Introduction

1

2 Pectins and arabinogalactan-proteins (AGPs) are the two major plant cell wall 3 glycopolymers rich in uronic acids (UA). These acidic UA residues, including 4 galacturonic acid (GalA) in pectins or glucuronic acid (GlcA) in AGPs, introduce 5 negative charges to these macromolecules at physiological conditions, affecting their 6 physiochemical properties and corresponding biological functions (Voragen et al., 2009, Lamport and Varnai, 2013). This is exemplified by the Ca<sup>2+</sup> binding capacity of these two 7 types of polymers and subsequent intramolecular and intermolecular formation of 8 9 calcium bridges that play important roles in wall integrity and cell-cell adhesion (Lopez-10 Hernandez et al., 2020, Pfeifer et al., 2020, Hyodo et al., 2013). 11 AGPs are distinctive glycoproteins that have large and highly branched polysaccharides attached to hydroxyproline (Hyp) and thus are often referred to as 12 13 hydroxyproline (Hyp)-rich glycoproteins (HRGPs). The Hyp-O-linked arabinogalactans 14 have a  $\beta$ -1,3-linked galactan backbone that is 1,6-substituted with  $\beta$ -galactosyl or  $\beta$ -1,6-15 galactan sidechains, and these sidechains are further decorated with arabinose (Ara), 16 GlcA, rhamnose (Rha), and fucose (Fuc) (Ellis et al., 2010, Tan et al., 2012, Classen et 17 al., 2019). This type of polysaccharide is referred to as type II arabinogalactan (AG) and is structurally distinct from type I and type III arabinogalactans, which have a  $\beta$ -1,4-18 linked or β-1,6-linked galactan backbone, respectively. The stable linkage between Hyp 19 20 and arabinogalactan not only makes it difficult to release and analyze an intact 21 arabinogalactan polysaccharide but also impedes efforts to sequence the polypeptides to 22 identify the corresponding genes for further functional analyses. 23 Pectins have three different structural elements: homogalacturonan (HG), 24 rhamnogalacturonan-I (RG-I), and rhamnogalacturonan-II (RG-II) (Mohnen, 2008, 25 Ropartz and Ralet, 2020, Kaczmarska, et al., 2022). HG is composed of a linear  $\alpha$ -1,4-26 linked GalA chain, while RG-II comprises an HG backbone decorated with six 27 sidechains, referred to as sidechains A to F (Barnes et al., 2021). In contrast, the 28 backbone of RG-I consists of repeats of -[2- $\alpha$ -L-Rhap-(1 $\rightarrow$ 4)- $\alpha$ -D-GalpA-1]-29 disaccharides, substituted with different sidechains, including  $\alpha$ -1,5-arabinan,  $\beta$ -1,4-30 galactan, and both type-I and type-II arabinogalactan (Harholt et al., 2010, Nascimento et 31 al., 2017). Some pectins are weakly associated with the cell wall and can be easily

32	extracted with oxalate and carbonate solutions. However, other pectins are tightly bound
33	to the wall and can only be released from the wall with endo-polygalacturonase (EPG)
34	treatment, yielding RG-I, RG-II, and oligogalacturonides (uronides) that can be separated
35	with size-exclusion chromatography (SEC) (York et al., 1986). Importantly, RG-II
36	always requires EPG treatment and cannot simply be extracted.
37	The existence of a pectin-AGP complex in the plant cell wall has been proposed
38	based upon numerous reports of co-purification of these macromolecules (Keegstra et al.,
39	1973, Yamada et al., 1987, Pellerin et al., 1995, Oosterveld et al., 2002, McKenna et al.,
40	2006, Leivas et al., 2016, Makarova and Shakhmatov, 2021). Previously, we provided
41	direct proof confirming that a covalent linkage is present between the reducing end GalA
42	of RG-I and the terminal rhamnosyl (Rha) residue of an AGP sidechain, -4-α-D-GalpA-
43	$(1\rightarrow 2)$ - $\alpha$ -L-Rha $p$ -, in a covalently linked arabinoxylan-pectin-arabinogalactan-protein 1
44	(APAP1) conjugate isolated from Arabidopsis suspension culture media (Tan et al.,
45	2013). The non-reducing-end of RG-I is further extended with repeats of HG and RG-I
46	oligomers, with the RG-I portion and AGP sidechain Ara residues substituted with
47	arabinoxylan. While we confirmed the covalent linkage between RG-I and AGP in
48	APAP1, which is secreted from the cell wall to the culture media, whether such a
49	structure is also present in the walls themselves is still an open question. To confirm this
50	hypothesis, an RG-I-AGP fraction was isolated from alcohol insoluble residues (AIR) of
51	Arabidopsis suspension cultured cells (Tan et al., 2013) and subjected to extensive
52	structural analysis. The present work reveals that APAP1-like structures do exist in plant
53	cell walls and describes the detailed structure of the RG-I-AGP. Using isolation,
54	composition, linkage, and NMR analyses of the glycans released from the RG-I-AGP
55	fraction by AGP-specific $\beta$ -1,3-galactanase and by RG lyase, we show that RG-I is
56	indeed linked to AGP. Quantitative analysis showed that this covalently linked RG-I-
57	AGP is the major component of the RG-I preparation released from the AIR by EPG. In
58	addition, the size of the RG-I linked to the AGPs proved to be a polysaccharide of around
59	41 KDa. This molecular weight and the calculated percentage of pectic sugars suggest an
60	RG-I-AGP is composed of one AGP covalently linked to two RG-I glycans.
61	

2. Materials and Methods

2.1. Preparation of RG-I enriched fraction

Suspension cultured wild type (WT) Arabidopsis cells were harvested using a sintered glass Buchner funnel. Alcohol-insoluble residues (AIR) were prepared from the cells as described (York et~al., 1986). The AIR sample was resuspended in cold water, titrated to pH 12.0 with 1 M NaOH on ice, and de-esterification was carried out overnight at 4 °C, followed by titrating to pH 5.2 with 1 M HCl. De-esterified AIR was dialyzed and lyophilized. An RG-I enriched fraction was prepared by treating de-esterified AIR with endo-polygalacturonase (EPG) (E-PGALPC, Megazyme) in 50 mM sodium acetate buffer (pH 5.2). The solubilized materials were filtered from the residues, dialyzed and lyophilized. The dried pectic materials were fractionated on a Superdex 75 column ( $10 \times 300$  mm, GE Healthcare Biosciences) eluted with 50 mM ammonium acetate buffer, which yielded three uronic acid-containing fractions. The three fractions have traditionally been referred to as RG-I, RG-II and uronides in order of decreasing molecular sizes (York et~al., 1986, Barnes et~al., 2021). Fractions were collected and lyophilized.

## 2.2. Purification of RG-I-AGPs from the RG-I preparation

The above RG-I preparation was dissolved in 50 mM Tris-HCl pH 7.0 and loaded on a 100-ml DEAE (GE Healthcare Biosciences) anion exchange column, which was washed with 100 ml 50 mM Tris-HCl pH 7.0 and eluted by a linear gradient from 50 mM Tris-HCl pH 7.0 to 2 M NaCl in 120 min. Eluted fractions were pooled, dialyzed against water for 2 days, and lyophilized. These materials were further purified on a PRP-1 reverse phase column (5  $\mu$ m, C-18, 4.1  $\times$  150 mm, Hamilton) using a gradient from 0.1% TFA in H<sub>2</sub>O to 80% (v/v) acetonitrile in 0.1% TFA in 100 min. The major fraction at 20 min was collected and lyophilized for further analysis.

## 2.3. Glycosyl composition and linkage analysis

Glycosyl composition analysis was performed by gas chromatography-mass spectrometry (GC-MS) of the trimethylsilyl (TMS) derivatives of the monosaccharide methyl glycosides generated from the samples by HCl methanolysis as described

previously (Santander et al., 2013). In brief, each sample was heated in 1 M methanolic 94 95 HCl for 18 h at 80 °C. The hydrolysate was dried, and the sample was derivatized with Tri-Sil<sup>TM</sup> HTP Reagent (Thermo Scientific) at 80 °C for 30 min. Following extraction 96 97 with hexane, GC-MS analysis of the TMS methyl glycosides was performed on an 98 Agilent 7890A GC interfaced to a 5975C MSD, using a Supelco Equity-1 fused silica capillary column (30 m × 0.25 mm ID). GC temperature program: 80 °C 2 min; 80 to 140 99 °C at 20 °C/min, hold for 2 min; 140 to 200 °C at 2 °C/min; 200 to 250 °C at 30 °C/min, 100 101 hold for 5 min. Split ratio: 100 to 1. MS source temperature: 230 °C; Quadrupole 102 temperature: 150 °C. Mass range: 50 – 550 Da. 103 Glycosyl linkage analysis was performed by GC-MS of the partially methylated 104 alditol acetate (PMAA) derivatives of the sample (Willis et al., 2013). Briefly, each 105 sample was suspended in DMSO and methylated using dimsyl potassium and 106 iodomethane (MeI) (Phillips and Fraser, 1981). The carboxylic acid methyl esters were 107 reduced using lithium aluminum deuteride in THF (80 °C, 8 h). The sample was re-108 methylated using MeI and hydrolyzed using 2 M TFA for 2 h at 120 °C. The hydrolysate 109 was reduced with NaBD<sub>4</sub>, followed by acetylation using acetic anhydride and TFA. The 110 resulting PMAAs were analyzed on an Agilent 7890A GC interfaced to a 5975C MSD; 111 separation was performed on a 30 m Supelco SP-2331 bonded phase fused silica capillary column. GC temperature program: 60 °C 1 min; 60 to 170 °C at 27.5 °C/min; 170 to 235 112 °C at 4 °C/min, hold for 2 min; 235 to 240 °C at 3 °C/min, hold for 12 min. Split ratio: 113 114 100 to 1. MS parameters were the same as above. 115 116 2.4. RG lyase expression and purification 117 A pET28a plasmid containing the BT4175 gene was a kind gift from Dr. Harry J. 118 Gilbert (Luis et al., 2018). Escherichia coli strain TUNER was transformed with the 119 plasmid and grown to mid-exponential phase before induction with 0.1 mM isopropyl β-120 D-galactopyranoside (IPTG), and the culture was grown for overnight at 16 °C and 160 121 rpm. The recombinant proteins were purified by using HisPur<sup>TM</sup> cobalt resin 122 (ThermoFisher) and dialyzed in HEPES sodium buffer (75 mM, pH 7.0). After dialysis, 123 the RG lyase was concentrated to 0.5 mg/ml using Amicon Ultra centrifugal filter device

124	(MWCO: 30 kDa, EMD Millipore). Protein concentration was measured with a		
125	NanoDrop 1000 spectrophotometer (ThermoFisher).		
126			
127	2.5. Release of glycans from the RG-I-AGPs with $\beta$ -1,3-galactanase or RG lyase		
128	The RG-I-AGPs (2 mg) were dissolved in 400 µl of 100 mM NaOAc, pH 5.2.		
129	Five microliters of <i>exo</i> -β-1,3-galactanase ( <i>C. thermocellum</i> , Gift from Megazyme) were		
130	added to the sample solution and the mixture was incubated at 37 °C for 24 h on a rotary		
131	shaker at 90 rpm.		
132	RG-I-AGPs (2 mg) were dissolved in 400 μl of 100 mM HEPES, pH 7.0. Ten μl		
133	of the RG lyase and 4.1 $\mu l$ of 1 M MnCl $_2$ were mixed with the sample. The digestion was		
134	carried on at 37 °C for 24 h on a rotary shaker at 90 rpm.		
135	For each digestion, the released glycans voided on a PRP-1 C18 reverse-phase		
136	column and separated from the remaining RG-I-AGPs using the above conditions for		
137	RG-I-AGP isolation.		
138			
139	2.6. Assay of xylan synthesis		
140	Enzyme reactions (20 $\mu$ l) consisted of 3 mM UDP-xylose (Carbosource) and 4 $\mu$ g		
141	xylan synthase KfXYS1 (Jensen et al., 2018) were proceeded in HEPES sodium buffer		
142	(50 mM, pH 7.0) at room temperature for 30 min. RG-I-AGP (10 $\mu$ g), APAP1 (10 $\mu$ g),		
143	xylopentaose (Megazyme, 50 $\mu M),$ and cellopentaose (Megazyme, 50 $\mu M)$ were used as		
144	the acceptor substrates. After 30 min, the production of UDP was measured by using		
145	UDP-Glo <sup>TM</sup> Glycosyltransferase Assay kit (Promega). Briefly, 5 μl of each reaction was		
146	mixed with 5 $\mu$ l UDP detection reagent in a 384-well plate (Greiner Bio-one). After 1 h		
147	incubation at room temperature, the luminescence was read in Synergy LX Microplate		
148	Spectrometer (BioTek).		
149			
150	2.7. Size determination of glycans by size exclusion chromatography with multi-angle		
151	light scattering and refractive index detection (SEC-MALS-RI)		
152	Glycans (0.8 mg) were dissolved in 400 $\mu$ l nanopure water and fractionated on an		
153	analytical Superdex 75 size exclusion column (10 $\times$ 300 mm, GE Healthcare		
154	Biosciences). The column was eluted with 50 mM ammonium formate at a flow rate of		

155 0.45 ml/min and monitored with an RI detector (Agilent). The molecular weight of each 156 fraction was estimated with a DAWN MALS detector (Wyatt technology). A series of 157 Dextran standards, of average sizes 167, 40, 10, and 1 kDa, were also separated on the same system to confirm the glycan sizes. The SEC-purified galactanase-released or RG 158 159 lyase-released glycans were lyophilized for NMR analysis. 160 161 2.8. Nuclear magnetic resonance (NMR) spectroscopy analysis 162 RG-I-AGPs (2 mg) or released glycans (500 µg) were dissolved in 150 µl of deuterium oxide. One microliter of 50 mM sodium 2,2-dimethyl-2-silapentane-5-163 sulfonate (DSS) in D<sub>2</sub>O was added as internal standard. <sup>1</sup>H and <sup>13</sup>C NMR spectra were 164 165 obtained at 25 °C with a Varian Inova 600 equipped with a 3 mm cryoprobe at the 166 Complex Carbohydrate Research Center. One- and two-dimensional NMR spectra were 167 collected as described previously (Tan et al., 2010). 168 169 3. Results 170 171 3.1. Structural analysis of the RG-I-AGPs derived from AIR 172 Our previous glycosyl composition and linkage analyses showed that the purified 173 RG-I-AGPs released from AIR of Arabidopsis suspension cultured cells by EPG consisted of 64.8 mol% Ara, 11.4 mol% GalA, 10.4 mol% Rha, and 13.4 mol% Gal, and 174 175 trace amount of Xyl, which were mostly pectic and AGP types of sugar residues (Tan et 176 al., 2013). To fully characterize their structures and understand their function in the cell wall, NMR experiments were carried out analyzing the structural elements of the purified 177 178 RG-I-AGPs (Figure 1 and Table A.1). Chemical shift assignments were based on a 179 heteronuclear single quantum coherence (HSQC) spectrum and published literature 180 reports (Zheng & Mort, 2008, Sun et al., 2010, Tan et al., 2004, 2010, 2013). Characteristic signals are summarized as follows: The <sup>13</sup>C/<sup>1</sup>H chemical shifts at 99.0/5.20 181 182 and 97.7/5.03 ppm represent the anomeric C/H of  $\alpha$ -2-Rhap and  $\alpha$ -GalpA residues, respectively. In addition, the <sup>13</sup>C/<sup>1</sup>H signals at 77.7/4.41 (GalpA-C/H4) and 70.4/4.88 183 184 ppm (GalpA-C/H5) corroborate that GalpA is 4-substituted, while signals at 77.5/4.14 185 (Rhap-C/H2) & 72.8/3.35 (Rhap-C/H4) ppm, and at 76.6/4.11 (Rhap-C/H2) & 81.5/3.84

(Rha*p*-C/H4) ppm substantiate the presence of 2-Rha*p* and 2,4-Rha*p* residues, respectively. These results confirm the existence of branched RG-I in this RG-I-AGP preparation. The intense <sup>13</sup>C/<sup>1</sup>H signals C/H5 of t-Ara*f* and 3-Ara*f* at 61.0/3.81,3.69 ppm and C/H5 of (2, and/or 3,)5-Ara*f* signals at 66.5/3.86,3.77 ppm, as well as the presence of 3,5-Ara*f*, 2,5-Ara*f*, & 2,3,5-Ara*f* in the glycosyl linkage data, suggest that the RG-I is substituted with branched 5-α-arabinan sidechains.

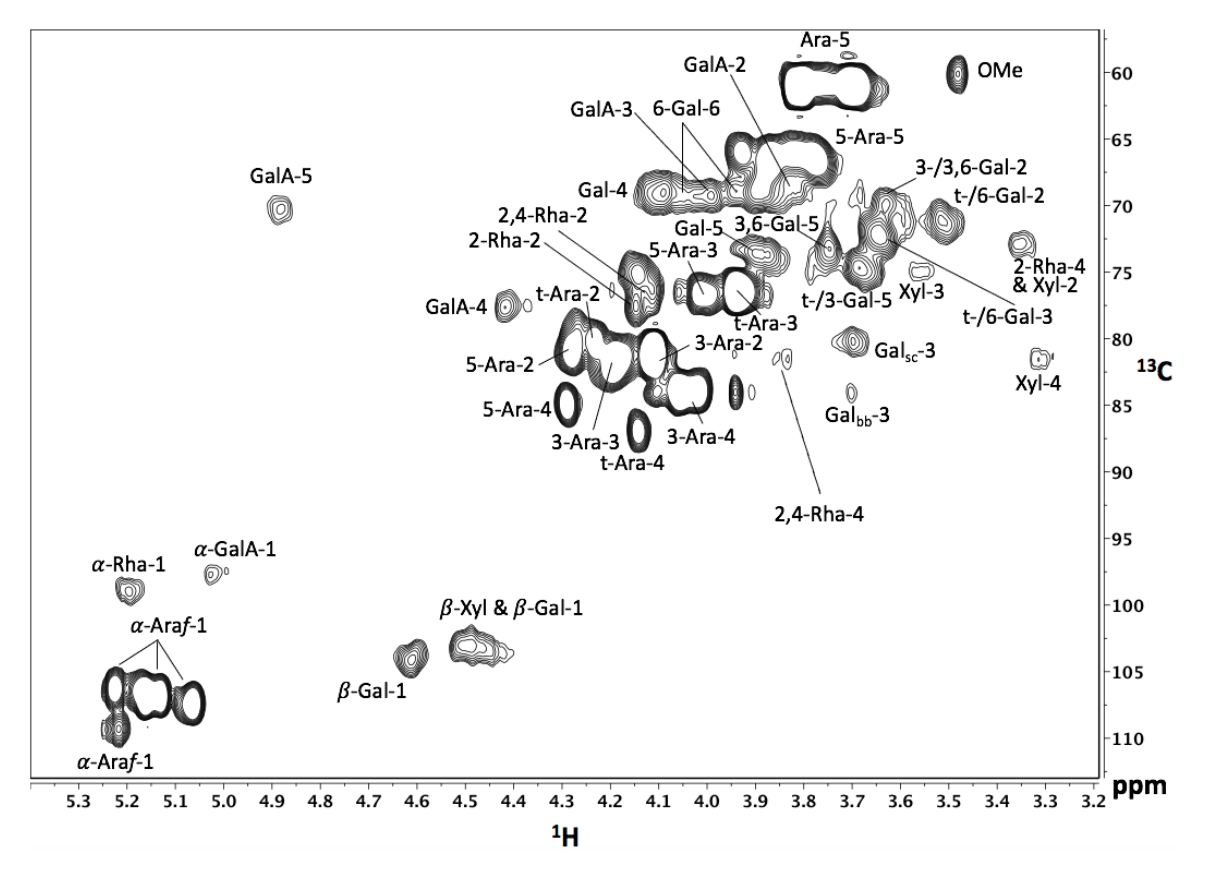


Figure 1. HSQC NMR spectrum of the intact RG-I-AGPs.

The chemical shifts confirmed the presence of RG-I and AGP types of structural elements. The spectrum was collected at 25 °C and referenced to DSS internal standard.

196

197 The distinctive  ${}^{13}\text{C}/{}^{1}\text{H}$  chemical shifts at 84.2/3.70 ppm and 80.3/3.69,

representing C/H3 of the branching 3,6-Gal*p* residues on the 1,3-galactan backbone (Gal<sub>bb</sub>) and on the 1,3-galactosyl sidechains (Gal<sub>sc</sub>), respectively, confirm the presence of type-II AG (Tan *et al.*, 2004, 2010). In addition, the unique <sup>13</sup>C/<sup>1</sup>H signals of Xyl*p* residues at 81.6/3.31 ppm suggest that some of the Xyl*p* residues are 4-*O*-methylated (Tan *et al.*, 2013). NMR analysis of the sample verified the presence of RG-I and type II

AG structural elements in the RG-I-AGP preparation, consistent with the structure depicted in Figure 2. However, direct evidence of the linkages between the RG-I and AG elements is still lacking since heteronuclear multiple bond correlation (HMBC) spectrum of polysaccharides as large as the RG-I-AGPs suffers from insufficient resolution and sensitivity. Data resolving these linkages are described further below.

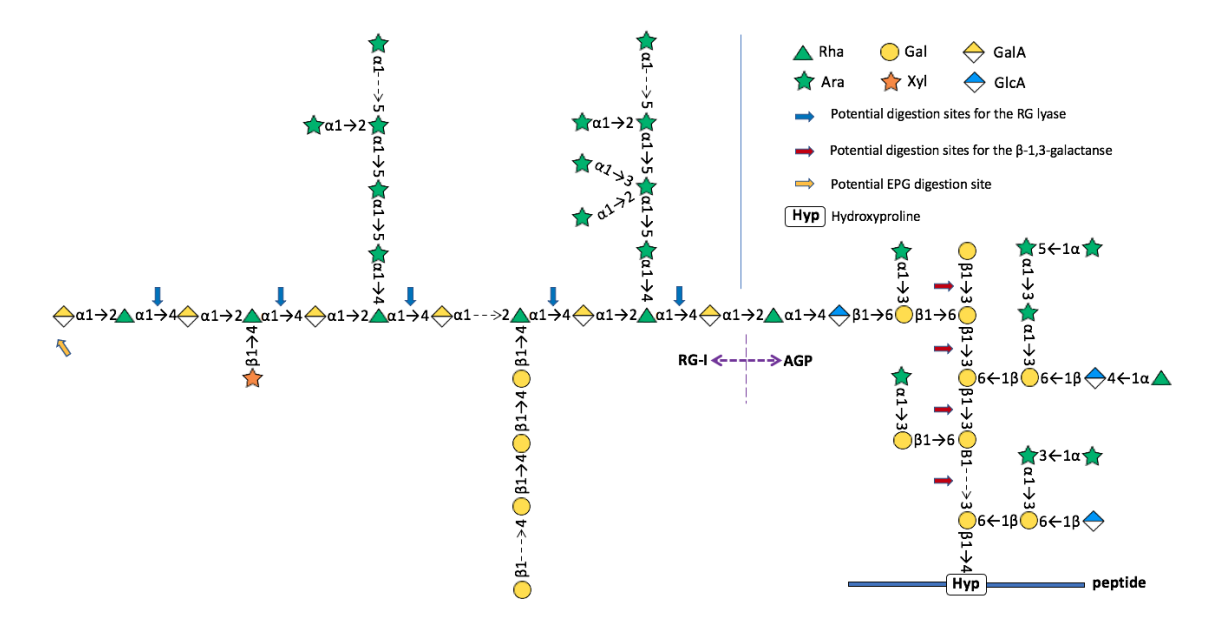


Figure 2. Scheme of the RG-I-AGPs isolated from AIR of Arabidopsis suspension cultured cells.

The  $\beta$ -1,3-galactanase can release a whole RG-I glycan with the AG sidechain residues, while the RG lyase can only produce RG-I fragments from the RG-I glycan.

## 3.2. Structure of glycans released by an exo- $\beta$ -1,3-galactanase

To confirm the linkage between the RG-I and AGP in the RG-I-AGP preparation, an AGP-specific *exo*-β-1,3-galactanase was used since this enzyme can sequentially liberate galactosyl residues (and the attached sidechains) from the non-reducing end of the AGP β-1,3-galactan backbone (Figure 2) (Tsumuraya *et al.*, 1990, Tryfona *et al.*, 2010, 2012). If the RG-I is covalently linked to AGP, digestion with this galactanase should generate fragments consisting of a reducing-end Gal (produced from the galactan backbone) and the attached AG sidechain with the covalently linked RG-I (see Figure 2).

Our analysis proved that such a fragment structure in fact exists in the galactanasegenerated glycans.

223

224

225

226

227

228

229

230

231

232

233

234

235

236

237

238

239

240

241

242

243

244

245

246

247

248

249

250

251

252

253

Specifically, after enzyme treatment, the released glycans were separated from the residual AGP conjugates by reverse phase chromatography (Figure A.1C). Glycosyl linkage analysis of the galactanase-released glycans gave significant percentages of partially methylated additol acetates (PMAAs) corresponding to 2-linked and 2,4-linked Rhap and 4-linked GalpA (Table 1), which are characteristic residues found in RG-I, in addition to the PMAAs coming from 3-Galp, 6-Galp, and 3,6-Galp, as well as the different Araf linkages, which are all typical AG residues. This confirms the existence of a highly branched RG-I structure in these β-1,3-galactanase-released glycans. This result supports the hypothesis that RG-I is covalently linked to AG in the RG-I-AGP preparation, as the AGP-specific enzyme can liberate RG-I from the preparation. NMR analysis of the released glycans confirms these linkage results (Figure 3 and Table A.2). A comprehensive chemical shift assignment was achieved based on a suite of two-dimensional (2D) NMR experiments summarized as follows: The proton resonances of each glycosyl residue were identified in a correlated spectroscopy (COSY) spectrum (Figure 3A) and a total correlation spectroscopy (TOCSY), and the corresponding carbon resonances were determined in an HSQC spectrum (Figure 3B). The glycosidic linkages of these glycosides, described in the following paragraph, were determined using an HMBC spectrum (Figure 3C). Specifically, like in intact RG-I-AGPs, the <sup>13</sup>C/<sup>1</sup>H signals at 98.8/5.20 ppm [2(,4)- $\alpha$ -Rhap-C/H1] and 97.6-97.7/5.01-5.03 ( $\alpha$ -GalpA-C/H1) ppm confirm the presence of  $2(4)-\alpha$ -Rhap and  $\alpha$ -GalpA (Figure 3B), respectively. Moreover, chemical shifts at 77.7/4.42 ppm ( $\alpha$ -GalpA-C/H4) in the HSQC spectrum suggest  $\alpha$ -GalpA residues are 4-linked, while those at 76.4/4.1 ppm (α-Rhap-C/H2) and 80.1/3.71 ppm ( $\alpha$ -Rhap-C/H4) verify that some  $\alpha$ -Rhap residues are 2,4-linked. These results are consistent with the linkage analysis, which showed that the RG-I glycans released by the AGP-specific galactanase are highly branched. H-H correlation between 4.53 and 3.63 ppm in Figure 3A also confirms the presence of β-GlcA, which was absent in the parent RG-I-AGP because of its low abundance in the whole large molecule (Figure 1). The corresponding anomeric C signal (103.0 ppm) is identified in the HSQC spectrum (Figure 3B). The chemical shifts at 92.3/5.25 & 96.3/4.58 ppm (Galp-C/H1) represent the  $\alpha$ - and

β-anomers of the reducing end Galp residue (Figure 3A), produced by the 1,3-galactanase
 cleavage.

Table 1. Glycosyl linkage analyses of β-1,3-galactanase and RG lyase released glycans
 from the RG-I-AGPs.
 After digestion, the oligosaccharides were desalted on a LH20 column and separated

from the rest of glycoproteins on a reverse-phase column as a void fraction.

Glycans released with		Glycans released with RG lyase	
Glycosyl Residue	Mol%	Glycosyl Residue	Mol%
		t-Rha <i>p</i>	0.8
2-Rhap	3.1	2-Rhap	10.0
4-Rhap	3.5	4-Rhap	0.7
2,4-Rha <i>p</i>	4.9	2,4-Rha <i>p</i>	3.8
		2,3,4-Rha <i>p</i>	24.3
		t-Gal <i>p</i> A	0.8
4-GalpA	13	4-GalpA	13.2
t-Araf	11.5	t-Araf	1.4
3-Araf	1.0	- -	
5-Araf	5.5	5-Araf	0.9
3,5-Ara <i>f</i>	0.9		
2,5-Ara <i>f</i>	2.3		
2,3,5-Araf	1.3		
		2,3,5-Araf	10.4
t-Galp	8.7	t-Gal <i>p</i>	3.3
3-Gal <i>p</i>	7.5		
6-Galp	13.8		
3,6-Gal <i>p</i>	13.9		
4,6-Gal <i>p</i>	1.2		
3,4,6-Gal <i>p</i>	1.5		
		2,3,4,6-Gal <i>p</i>	20.9
4-GlcpA	2.9		
3,4-Glc <i>p</i> A	1.6		
t-Xylp	1.4		
		4-Xyl $p$	0.9
		2,3,4-Xyl <i>p</i>	1.2
2-Manp	0.6	• -	
•		t-Glcp	0.9
		4-Glcp	4.3
		2,3,4,6-Glc <i>p</i>	2.2

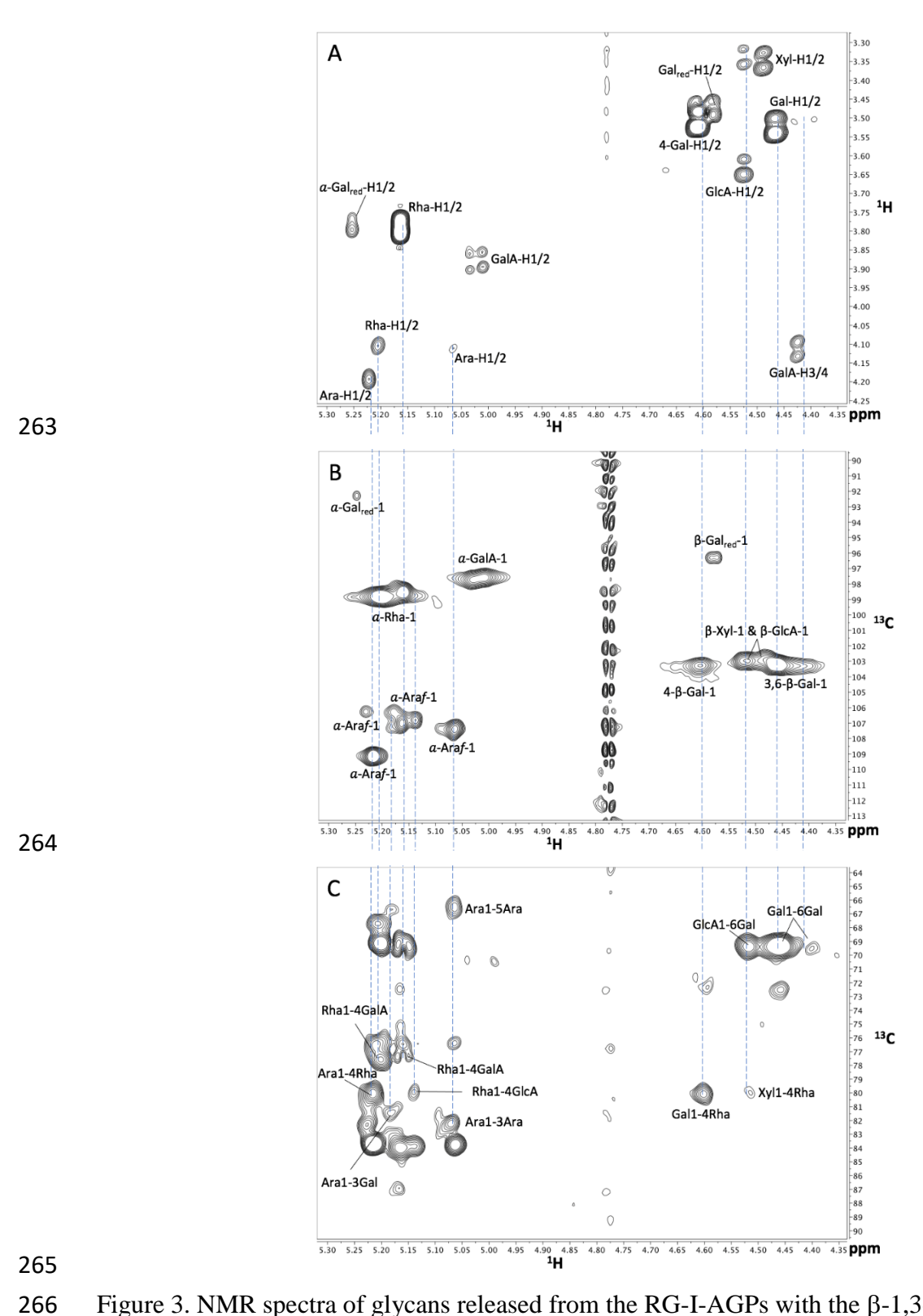


Figure 3. NMR spectra of glycans released from the RG-I-AGPs with the  $\beta$ -1,3-galactanase.

268 A. COSY spectrum, B. HSQC spectrum, C. HMBC spectrum. The structural elements in 269 the spectra confirm the released glycans are RG-I with different sidechains. The spectra 270 were collected at 25 °C and referenced to DSS internal standard. 271 272 The HMBC spectrum provided linkage information between different structural 273 elements in the AGP-specific galactanase-released glycans (Figure 3C). The β-3,6-Gal 274 residues with anomeric C/H at 103.0/4.4 ppm are from the sidechain  $\beta$ -Galp residues 275 substituted at position-3 by  $\alpha$ -Araf residues, as evidenced by the correlation between  $\alpha$ -276 Araf-H1 (5.19 ppm) and β-Galp-C3 (81.8 ppm). Correlations between sidechain β-Galp-277 H1 (4.46 or 4.39 ppm) and  $\beta$ -Galp-C6 at 69.3 ppm support the  $\beta$ -Galp-(1 $\rightarrow$ 6)- $\beta$ -Galp 278 linkage, while those between β-GlcpA-H1 (4.53 ppm) and β-Galp-C6 (69.3 ppm) 279 confirm the  $\beta$ -GlcpA-(1 $\rightarrow$ 6)- $\beta$ -Galp substitution. These structural elements are consistent 280 with a structural element  $\beta$ -GlcpA-(1 $\rightarrow$ 6)-[ $\alpha$ -Araf-(1 $\rightarrow$ 3)-]- $\beta$ -Galp-(1 $\rightarrow$ 6)-Gal<sub>reducing</sub> 281 produced from typical AGPs by the galactanase (Figure 2) (Tan et al., 2014, 2010, 282 Tryfona *et al.*, 2010). 283 The linkages within the RG-I structure are confirmed by the correlations in the 284 HMBC spectrum (Figure 3B). The correlations of  $\alpha$ -Rhap-H1 (5.20 or 5.16 ppm) to  $\alpha$ -285 GalpA-C4 (77.7 ppm) support the  $\alpha$ -Rhap-(1 $\rightarrow$ 4)- $\alpha$ -GalpA linkages. The arabinan is corroborated by the correlations between α-Araf-H1 (5.06 ppm) & α-Araf-C5 (67.8 ppm) 286 287 and α-Araf-H1 (5.06 ppm) & α-Araf-C3 (83.7 ppm). The RG-I sidechain substitutions 288 are supported by correlations between α-Araf-H1 (5.22 ppm) & α-Rhap-C4 (80.1 ppm), 289 β-Galp-H1 (4.61 ppm) & α-Rhap-C4 (80.1 ppm), and β-Xylp-H1 (4.53 ppm) & α-Rhap-290 C4 (80.1 ppm), which establish the attachment of 1,5-arabinan, 1,4-galactan, and t-4-O-291 Me- $\beta$ -Xylp to the RG-I Rhap residues, respectively. We did not observe 4-linked Xylp in 292 the NMR spectra and in the glycosyl linkage analysis (Table 1), and together with the 293 HMBC correlation between Xyl H1 and Rha-C4, this suggests that the xylosyl sidechains 294 consist of a single residue. These results affirm that the RG-I portion of the RG-I-AGP 295 preparation is highly decorated with different substituents. In general, 2-O-glycosylated α-Rhap residues show a chemical shift displacement 296

relative to the  $\alpha$ -Rhap anomeric C/H from 102/4.80 ppm (t- $\alpha$ -Rhap) to ~99/~5.1 ppm (2-

 $\alpha$ -Rhap) (Tan et~al., 2004, 2010, 2013). Thus, the signal at 5.14/99.6 ppm is likely from a 2- $\alpha$ -Rhap. An HMBC correlation between its anomeric proton and a carbon signal at 79.9 ppm (C4 of  $\beta$ -GlcpA) demonstrates the presence of a 2- $\alpha$ -Rhap-(1 $\rightarrow$ 4)- $\beta$ -GlcpA linkage, which further supports that the AGP sidechain Rha residues were 2-O-substituted. Considering that the glycans, with RG-I and the -2- $\alpha$ -Rhap-(1 $\rightarrow$ 4)- $\beta$ -GlcpA- structural elements, were released from the RG-I-AGP complex by the galactanase and enriched by SEC separation (Figure 4A), the results support the attachment of RG-I to the O2 of the sidechain Rhap of AGP (Figure 3C) (Tan et~al., 2013), further confirming our hypothesis that RG-I is covalently linked to AGP.

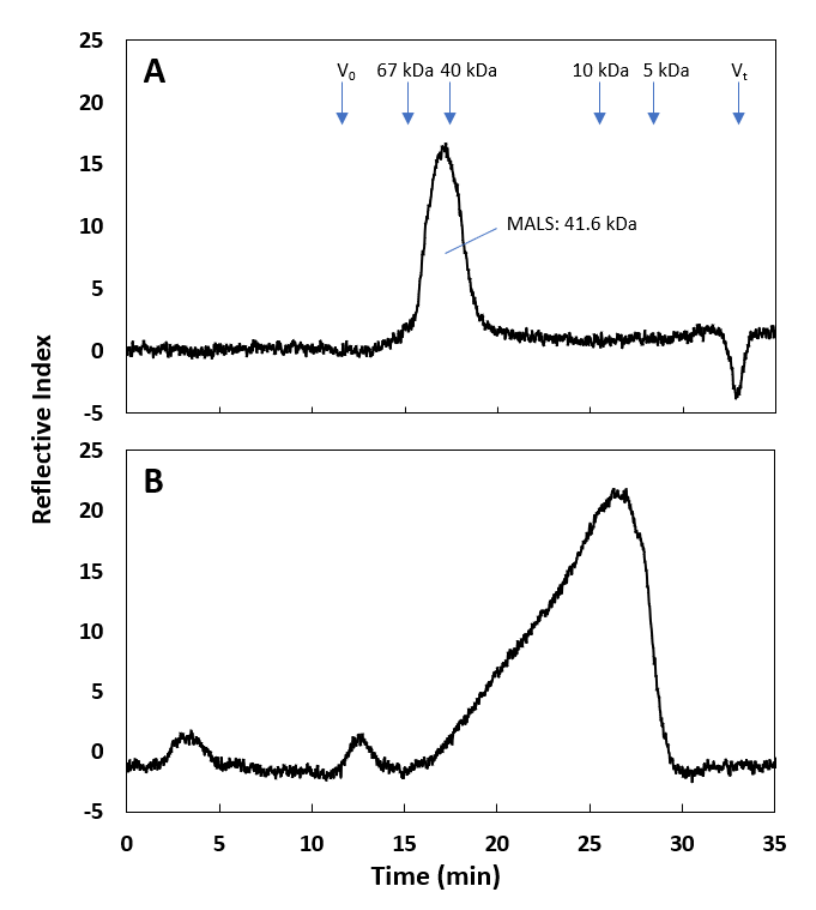


Figure 4. HPLC chromatograms of glycans released from the RG-I-AGPs on SEC-MALS-RI.

Glycans released with  $\beta$ -1,3-galactanase (A) and with RG lyase (B) were separated on a Superdex 75 size-exclusion column and monitored with MALS-RI detectors. The

molecular weights of all dextran standards were labeled at the corresponding retention times in panel A.

315

316

317

318

319

320

321

322

323

324

325

326

327

328

329

330

331

332

333

334

335

336

313

314

3.3. The structure of glycans released by rhamnogalacturonan lyase

To obtain more structural information of the RG-I portion of the complex, the RG-I-AGP preparation was treated with rhamnogalacturonan (RG) lyase BT4175 (Luis et al., 2018), and the released glycans were separated from the remaining RG-I-AGPs using a C18-reverse phase column (Figure A.1D). Glycosyl linkage analysis of these released glycans, which were eluted from the column in the void volume, showed the presence of typical RG-I type glycosyl linkages (Table 1), although certain glycosyl residues were under-methylated. Further NMR analysis was carried out to secure the RG-I structure of these glycans (Figure 5 and Table A.3). The chemical shift assignment was based on a total correlation spectroscopy (TOCSY) spectrum and an HSQC spectrum, in addition to the NMR results in above section 3.2, and assignments from the literature (Mutter et al., 1998, Deng et al., 2006). In contrast to the galactanase digest, no residues originating from AGP were detected. The HSQC spectrum confirmed the RG-I type glycosyl residues in the sample, including the backbone  $\alpha$ -2-Rhap,  $\alpha$ -2,4-Rhap, and  $\alpha$ -4-GalpA residues, as well as the  $\alpha$ -t-Araf,  $\alpha$ -3-Araf, and  $\alpha$ -5-Araf residues,  $\beta$ -4-Gal residues, and β-t-Xyl residues on the sidechains. The characteristic <sup>13</sup>C/<sup>1</sup>H chemical shifts at 107.5/5.79  $(^{4,5}\Delta\text{-Gal}p\text{A-C/H4})$  and 65.8/4.31  $(^{4,5}\Delta\text{-Gal}p\text{A-C/H3})$  ppm verified the non-reducing ends of the released glycans are  $^{4,5}\Delta$ -GalpA (Mutter et al., 1998, Deng et al., 2006), generated by the RG lyase. No AGP linkages such as  $\beta$ -3-Galp,  $\beta$ -3,6-Galp, and  $\beta$ -4-GlcpA were identified in this sample.

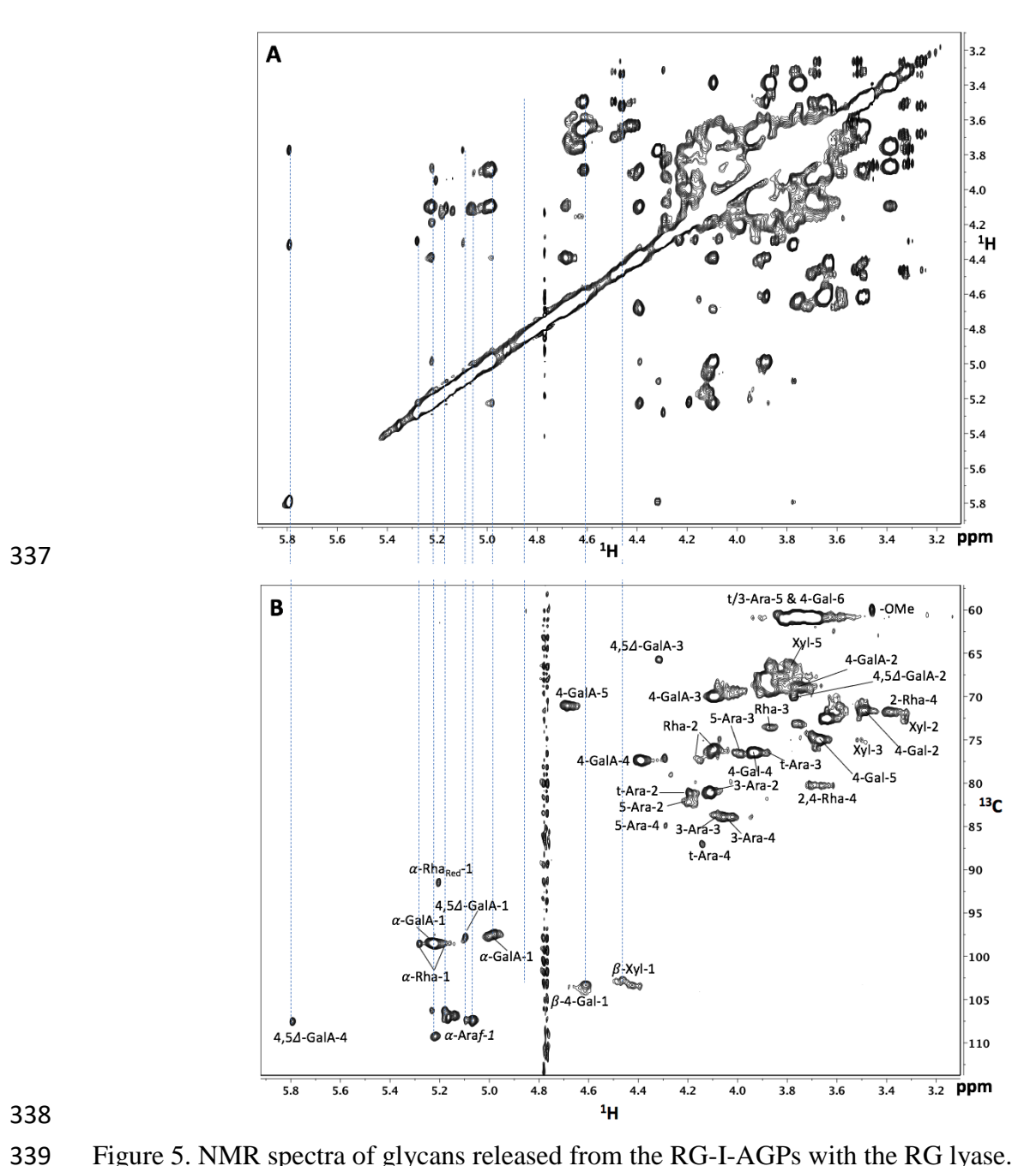


Figure 5. NMR spectra of glycans released from the RG-I-AGPs with the RG lyase.

A. TOCSY spectrum, B. HSQC spectrum. The chemical shifts confirm the enzyme released glycans are RG-I fragments with different sidechains. The spectra were collected at 25 °C and referenced to DSS internal standard.

3.4. SEC-MALS-RI reveals size of the RG-I glycans appended to the RG-I-AGPs

The molecular weight of the RG-I glycans attached to the AGPs was determined by SEC-MALS-RI. Specifically, Superdex 75 SEC-MALS-RI was used to measure the

347 molecular weight using a MALS detector directly and an RI detector (Figure 4A) with 348 dextran standards. The released pectic glycans showed a short retention time (16 to 18.5) 349 min, centered at 17.6 min) on the SEC column. The MALS detector measured the 350 average molecular weight as 41.6 kDa, while comparison to the dextran standards 351 suggested the molecular weight is close to 40 kDa in good agreement with the MALS 352 measurement. Thus, the average molecular weight of the RG-I glycans in the RG-I-AGP 353 complexes is about 41 kDa. 354 355 3.5. Measuring the size of glycans released by a rhamnogalacturonan lyase The branching Rha residues, 2,4-Rha, account for 42.6% of the total Rha in the 356 357 galactanase-released RG-I glycans (Table 1), indicating the RG-I is highly branched. 358

Despite this high degree of branching, one treatment with the RG lyase can remove RG-I

glycans corresponding to one third of the starting weight of RG-I-AGP, confirming that

the RG lyase can cleave the RG-I backbone even in the presence of sidechains. To

measure the molecular weight of RG-I glycans released by the RG lyase, we used the

Superdex 75 SEC-MALS-RI system (Figure 4B). The SEC chromatogram showed a

broad profile with retention time ranging from 16 to 29 min, with measured sizes ranging

from 5 to 41 kDa by the MALS detector and RI dextran standards. The SEC profile also

showed an asymmetric peak distribution with higher abundance of materials with lower

molecular weight, correspondingly producing a range of short RG-I oligosaccharides to

long RG-I glycans (41 kDa) that are close to the full-length RG-I glycans (41 kDa)

released by the galactanase from the RG-I-AGPs. This result confirms the accuracy of the

measured sizes of the RG-I in the RG-I-AGPs.

370 371

372

373

374

375

376

377

359

360

361

362

363

364

365

366

367

368

369

## 3.6. RG-I-AGP is the major component of the RG-I preparation

To measure how much of the traditional RG-I preparation (Figure A.1A) consisted of RG-I-AGP conjugates, we chose the following experimental approach (Figure 6): A one-step EPG treatment released about 245.8 mg [9.8% (w/w)] of materials from 2.5 g of the AIR residues, in which 95.9 mg of the materials [39% (w/w)] became insoluble after dialysis and lyophilization. After separation of the soluble portion (149.9) mg) of the EPG-released materials on a Superdex 75 size exclusion column (Fig A.1A),

the largest molecular weight fraction (retention time 16-20 min), which has been traditionally named RG-I, was collected and freeze-dried (105.7 mg). The yield of traditional RG-I prep from the AIR was 4.2% (w/w).

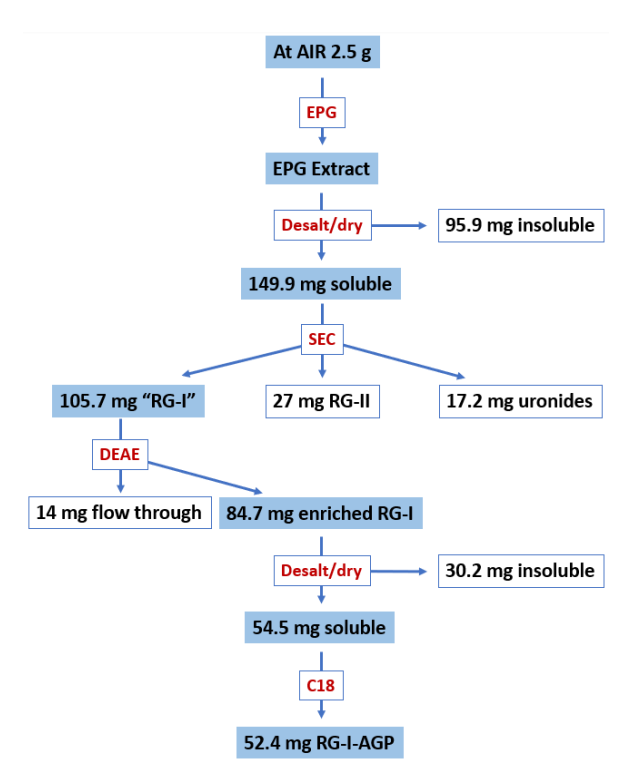


Figure 6. Yields of materials during the steps of RG-I-AGPs purification.

At AIR: alcohol insoluble residues prepared from Arabidopsis suspension cultured cells; SEC: size-exclusion chromatography.

This traditional RG-I prep was further purified on a DEAE anion exchange column to remove neutral glycan components (Fig A.1B) and reverse-phase column (Tan *et al.*, 2013) to enrich the RG-I-AGPs. The results showed that the DEAE purification enriched 84.7 mg [80.1% (w/w)] of RG-I prep from the 105.7 mg of traditional RG-I prep (Figure 6), in which 30.2 mg of materials, accounting for 36% w/w of the enriched RG-I prep, became insoluble after lyophilization. Further reverse-phase purification yielded 52.4 mg of the final RG-I-AGP, which accounted for 96% (w/w) of the soluble DEAE-purified RG-I prep (54.5 mg), 69.4% (w/w) of the soluble traditional RG-I [75.5 mg (105.7-30.2 mg)], and 2.1% (w/w) of the AIR. Therefore, the traditional RG-I prep (105.7

mg) from the AIR of Arabidopsis suspension cultured cells mainly comprises covalently linked RG-I and AGPs [52.4 mg (49.6%, w/w)].

398

399

400

401

402

403

404

405

406

407

408

409

410

411

412

413

414

415

416

417

418

419

420

421

422

423

424

425

426

396

397

## 4. Discussion

In this work, we showed that the EPG-released RG-I from the AIR preparation of cultured wild-type Arabidopsis cells consisted largely of RG-I that was covalently attached to AGP, i.e. RG-I-AGP. Structural evidence for this RG-I-AGP attachment was provided by the AGP-specific  $\beta$ -1,3 galactanase release of RG-I glycans and the identification of the linkage between RG-I and AGP sidechain Rha in the HMBC NMR spectrum of the galactanase-released glycans. Furthermore, it was demonstrated that RG-I-AGP was the major molecule present in the RG-I preparation, and that the RG-I polysaccharide was relatively large in size, i.e. 41 kDa. The yield of the RG-I-AGPs (52.4 mg) from the soluble RG-I prep (54.5 mg) suggests that about 96% (w/w) of the soluble RG-I is covalently attached RG-I-AGPs, and the purified RG-I-AGPs (52.4 mg) account for 69.4% (w/w) of the soluble traditional RG-I preparation [75.5 mg (105.7-30.2 mg)] (Figure A.1A). Moreover, glycosyl composition analysis of the water-insoluble RG-I preparation (30.2 mg) after DEAE column showed that these materials are also mainly composed of RG-I and AGP types of glycosyl residues (Table A.4). However, the structure of this insoluble fraction still needs to be elucidated, and we have recently developed methods (Black et al., 2019, Ndukwe et al., 2020) for the structural characterization of insoluble polysaccharides that we plan to exploit for this purpose. Traditionally, we designate the first or the largest-sized SEC fraction of the EPG released cell wall materials as RG-I (Figure A.1A). Here, we characterized the majority of this traditional RG-I as covalently linked RG-I-AGP. In recent years, many cell wall specific carbohydrate degrading enzymes have been discovered (Ndeh et al. 2017, Cartmell et al., 2018, Ndeh and Gilbert 2018, McKee et al., 2021). This provides powerful analytical tools for the selective cleavage of individual linkages, as well as structural information of targeted wall components. Dupree, Tsumuraya, and colleagues (Tryfona et al., 2010, 2012, Shimoda et al., 2014) successfully characterized some AGP structures by making use of different AGP-specific

enzymes, including exo- $\beta$ -1,3-galactanase,  $\alpha$ -L-arabinofuranosidase,  $\beta$ -glucuronidase,

and endo- $\beta$ -1,6-galactanase and by analyzing the products of these enzymes with gel electrophoresis and mass spectrometry (MS) techniques. These enzymes, especially the exo- $\beta$ -1,3-galactanase that can notably trim the core AG structures, enable the analysis of AG sidechains of low abundances that cannot be detected by traditional MS and NMR analyses.

Here, the release of RG-I glycans from the RG-I-AGPs by the AGP-specific  $\beta$ -1,3-galactanase provided strong evidence supporting that RG-I is covalently attached to the sidechains of AGPs. The galactanase-catalyzed cleavage also significantly simplified the RG-I structural analysis by removing most of the AG portion of the RG-I-AGPs from the released RG-I glycans. This feature also makes it possible to apply this enzyme directly on cell walls or AIR to release RG-I or pectin as a complementary approach in place of EPG treatment. Both glycosyl composition and linkage analyses as well as NMR results demonstrate that the RG-I backbone is decorated with  $\alpha$ -1,5-arabinan,  $\beta$ -1,4-galactan, t- $\beta$ -Xyl, and t-4- $\theta$ -Me- $\theta$ -Xyl sidechains. The relative molar ratio of 2-Rha and 2,4-Rha (1:1.6) suggest that the Rha residues on the RG-I backbones are highly substituted with those sidechains. It is noteworthy that the released RG-I did not contain type II AG sidechains, raising the question whether the type II AG that has traditionally been viewed as RG-I sidechains in reality originates from the AG portion of RG-I-AGPs also in other plants. We will need to isolate and characterize RG-I-AGPs from several additional species to evaluate whether this is generally the case.

APAP1 and RG-I-AGPs are pectic AGPs with reducing ends of pectin and RG-I covalently linked to AGPs, respectively. In the case of APAP1, which was secreted into the culture media from the walls, the calculated pectin length is short with an average 4-GalA/4-GlcA ratio of ~6:1, i.e. one pectin glycan has ~6 GalA residues if all GlcA-containing AG sidechains are substituted with pectin glycans (Tan *et al.*, 2013). Here, the RG-I-AGPs were released from the AIR by EPG digestion, which would cleave the HG portions of pectin molecules and liberate the covalently attached RG-II, RG-I (Harholt *et al.*, 2010), and RG-I-AGP located at the reducing end of pectin/RG-I. The long RG-I glycans (~41 kDa) of the RG-I-AGP consisted of several hundred glycosyl residues. We found that the glycoconjugates of which the RG-I-AGPs are part, and which may also comprise the covalently linked HG and RG-II (and even covalently attached xylan chains

- as presented in APAP1) cannot be extracted from the cell wall but require digestion by
- 459 EPG. This indicates that the RG-I-AGPs in their context as part of a larger
- 460 glycoconjugate are tightly associated in the cell wall. This feature fits our hypothesis that
- was stated in the previous paper; namely that "APAP1 with longer pectin and
- arabinoxylan chains may exist in the cell walls and that such macromolecules are highly
- crosslinked and interwoven in the walls and thus cannot be released into the culture
- 464 media" (Tan et al., 2013).
- Arabinosylation is a major modification of both RG-I and AGP. The arabinan
- sidechain of RG-I is composed of a 1,5-linked α-L-arabinan backbone, which is usually
- 467 further 2-O and/or 3-O substituted with α-L-arabinosyl residues (Mohnen, 2008, Luis et
- 468 al., 2018). AGP galactan arabinosylation includes formation of t- $\alpha$ -L-Araf-(1 $\rightarrow$ 5)- $\alpha$ -L-
- Araf- $(1 \rightarrow 3)$ - $\alpha$ -L-Araf- $(1, \alpha$ -L-Araf- $(1 \rightarrow 3)$ - $\alpha$ -L-Araf- $(1, \alpha$ -Araf- $(1, \alpha$
- are 3-O linked to AG sidechain Gal (Defaye and Wong, 1986, Gane et al., 1995, Tan et
- 471 *al.*, 2004, 2010, Knoch *et al.*, 2014). Therefore, 5-Araf, as well as 2,5-Araf and 3,5-Araf,
- are the main Ara linkages in RG-I, while 5-Araf is a minor Ara linkage in AGP and even
- absent in some AGPs (Tryfona et al., 2010, Cartmell et al., 2018, Ndeh and Gilbert,
- 474 2018, Munoz-Munoz et al., 2021). In the case of the present RG-I-AGP, which is
- 475 composed of 64.8 mol% Ara, 11.4 mol% GalA, 10.4 mol% Rha, and 13.4 mol% Gal (Tan
- et al., 2013), 5-Araf in the AGP portion should be no more than the mol% of 3-Araf,
- which is 0.4%. Most 5-Araf [>8.0% (8.4-0.4 mol%)] is from the RG-I portion. With other
- 478 types of RG-I Araf linkages such as 1.9% 3,5-Araf, 4.2% 2,5-Araf, & branching t-Araf
- 479 [substituting 3-O (1.9%) & 2-O (4.2%) on the 3,5- & 2,5-Araf, respectively], at least
- 480 20.2% (8.0+1.9+4.2+1.9+4.2) out of all 35.3% Ara linkages is on RG-I, i.e. at least
- 481 57.2% (20.2/35.3) of Ara residues (37.1 mol%) are from RG-I sidechain arabinan (Tan *et*
- 482 *al.*, 2013).
- 483 Almost all of the Rha (10.2 mol%) is pectic 2-, 2,3-, & 2,4-Rha (Tan *et al.*, 2013).
- In addition, based on a 3:1 relative ratio of anomeric signals of Araf:Galp in the HSQC
- spectrum of the RG lyase released RG-I glycans (Figure 5B), the 4-Galp attributes to
- about 10.8 mol% (one third of 32.4 mol% of RG-I arabinosyl residues) of total sugars in
- the RG-I-AGP. Thus, the RG-I accounts for at least 69.5 mol% (11.4% GalA + 10.2%)
- 488 Rha + 37.1% Ara + 10.8% Gal) of carbohydrates in the RG-I-AGP, and the other 30.5

mol% of total carbohydrates (27.7 mol% Ara + 2.6 mol% Gal + 0.2 mol% Rha) are from the AG portion. Considering the molecular weight of the RG-I-AGP (~120 kDa), the attached RG-I (≪41 kDa), and the matured polypeptide of the AGP (10.8 kDa), this suggests that one RG-I-AGP molecule consists of one molecule of AGP and two molecules of RG-I (the calculation is presented in Figure A.3), i.e. one AGP can covalently link two individual RG-I. It indicates that *in vivo* one AGP can crosslink two pectin glycans in the cell wall. Therefore, AGPs involved in such complex structures play an important role in crosslinking pectin glycans for a functional wall structure.

The attachment of RG-I to AGP raises an important question regarding the biosynthesis of such a complex structure. All identified glycosyltransferases (GTs) involved in pectin and AG biosynthesis are Golgi-localized. Classic AGPs, such as AtAGP57, are anchored to the Golgi membrane via a C-terminal GPI anchor during glycosylation. Since both GTs and AGPs are Golgi membrane-anchored, it is likely that RG-I-AGP synthesis occurs inside the Golgi. In this context, t-Rha on AGP would serve as the initiation site for addition of RG-I. This is accomplished by the Golgi-localized RG-I specific enzymes rhamnosyl transferase and galacturonic acid transferase (Figure A.2A).

According to our previous work (Tan *et al.*, 2013), APAP1, which is isolated from the culture medium, is decorated with xylan sidechains with an average degree of polymerization (DP) of 11. However, we have observed that the RG-I of RG-I-AGP from the cell wall characterized here has only monomeric Xyl and 4-*O*-methylated Xyl residues as sidechains. Some other reported pectin-AGP complexes also contained a small amount of Xyl (Saulnier & Brillouet, 1988, Ryden & Selvendran, 1990, Pellerin *et al.*, 1995, Oosterveld *et al.*, 2002, Duan *et al.*, 2004, Nergard *et al.*, 2005). The xylan DP differences between the reported pectic AGPs and the common presence of Xyl in the pectic AGPs raise the following questions: Are these minor Xyl moieties on RG-I the initiation sites for xylan elongation or addition? What is the function of 4-*O*-methylation of Xyl in RG-I-AGPs? Does it serve as the terminating signal for xylan elongation? Although xylan synthase and UDP-Xyl were unable to elongate the xylosyl sidechains on the RG-I-AGP (Figure A.4) *in vitro*, it is reasonable to expect that the xylan endotransglycosylase from plant cell wall (Johnston *et al.*, 2013, Frankova and Fry, 2020)

520 will be able to accomplish this chain elongation by adding xylan fragments hydrolyzed 521 from wall xylan onto the 4-O position of the t-Xyl (Figure A.2B). This xylan elongation 522 process on structures like RG-I-AGPs catalyzed by wall endotransglycosylation may 523 allow the formation of crosslinks between pectin and xylan in the wall in vivo. 524 Undoubtedly with more carbohydrate-specific enzymes, such as enzymes that can 525 cleave 4-β-GlcA with the directly linked RG-I from the RG-I-AGPs, and more powerful 526 analytical probes and tools, such as an antibody that recognize the specific  $-\alpha$ -GalpA-527  $(1\rightarrow 2)-\alpha$ -Rhap- $(1\rightarrow 4)-\beta$ -GlcpA- $(1\rightarrow 6)-\beta$ -Galp- linkage between RG-I and AGPs, we 528 will be able to track when and where RG-I and AGPs start to covalently link in planta. 529 When we understand how these macromolecules are synthesized, the role of such 530 complex structures in plant cell wall architecture will be revealed. 531 532 5. Conclusions 533 The RG-I preparation released from the AIR of Arabidopsis suspension cultured 534 cells are mainly composed of covalently linked RG-I and AGPs. The RG-I portion is 535 highly substituted with branched  $\alpha$ -1,5-arabinan,  $\beta$ -1,4-galactan, and single  $\beta$ -Xyl or 4-536 O-Me-β-Xyl residues. The RG-I glycans have an average molecular size of 41 kDa, 537 suggesting one AGP can crosslink two RG-I glycans. 538 539 **CRediT Authorship Contribution Statement** 540 LZ, BU, IB, JG, LT: Formal analysis; LT: conceptualization, investigation, original draft; 541 LT, CH, & PA: writing, review, funding acquisition. All authors: revision. 542 543 **Declaration of Competing Interest** 544 The authors declare that they have no competing interests. 545 Acknowledgements 546 547 LT thanks Dr. Vincent McKie from Megazyme for kindly providing the β-1,3-548 galactanase from C thermocellum. The authors acknowledge Dr. Russell Carlson for 549 critical review of this manuscript. This work was supported by the U.S. Department of

Energy, Office of Science, Basic Energy Sciences, Grant number DE-SC0015662.

551

## References

- Barnes, W.J., Koj, S., Black, I.M., Archer-Hartmann, S.A., Azadi, P., Urbanowicz, B.R.,
- Pena, M.J., O'Neill, M.A. (2021) Protocols for isolating and characterizing
- polysaccharides from plant cell walls: a case study using rhamnogalacturonan-II.
- 557 Biotechnol, Biofuels, 14: 142.
- Black, I., Heiss, C., Azadi, P. (2019) Comprehensive monosaccharide composition
- analysis of insoluble polysaccharides by permethylation to produce methyl alditol
- derivatives for gas chromatography/mass spectrometry. Anal. Chem. 91: 13787-13791.
- 561 Cartmell, A., Munoz-Munoz, J., Briggs, J.A., Ndeh, D.A., Lowe, E.C., Basle, A.,
- Terrapon, N., Stott, K., Heunis, T., Gray, J., Yu, L., Dupree, P., Fernandes, P.Z., Shah, S.,
- Williams, S.J., Labourel, A., Trost, M., Henrissat, B., Gilbert, H.J. (2018) A surface
- 564 endogalactanase in Bacteroides thetaiotaomicron confers keystone status for
- arabinogalactan degradation. Nat. Microbiol. 3: 1314-1326.
- Classen, B., Baumann, A., Utermoehlen, J. (2019) Arabinogalactan-proteins in spore-
- producing land plants. Carbohydr. Polym. 210: 215-224.
- Defaye, J., & Wong, E. (1986) Structural studies of gum arabic, the exudate
- polysaccharide from Acacia senegal. Carbohydr. Res. 150: 221-231.
- 570 Deng, C., O'Neill, M.A., York, W.S. (2006) Selective chemical depolymerization of
- 571 rhamnogalacturonans. Carbohydr. Res. 341: 474-484.
- 572 Duan, J., Zheng, Y., Dong, Q., Fang, J.N. (2004) Structural analysis of a pectic
- polysaccharide from the leaves of Diospyros kaki. Phytochemistry 65: 609-615.
- 574 Ellis, M., Egelund, J., Schultz, C.J., Bacic, A. (2010) Arabinogalactan-proteins: key
- regulators at the cell surface? Plant Physiol. 153: 403-419.
- 576 Frankova, L., & Fry, S.C. (2020) Activity and action of cell-wall transglycanases.
- 577 Methods Mol. Biol. 2149: 165-192.
- 578 Gane, A.M., Craik, D., Munro, S.L., Howlett, G.J., Clarke, A.E., Bacic, A. (1995)
- 579 Structural analysis of the carbohydrate moiety of arabinogalactan-proteins from stigma
- and styles of Nicotiana alata. Carbohydr. Res. 277: 67-85.
- Harholt, J., Suttangkakul, A., Scheller, H.V. (2010) Biosynthesis of pectin. Plant Physiol.
- 582 153: 384-395.

- 583 Hyodo, H., Terao, A., Furukawa, J., Sokamoto, N., Yurimoto, H., Satoh, S., Iwai, H.
- 584 (2013) Tissue specific localization of pectin-Ca<sup>2+</sup> cross-linkages and pectin methyl-
- esterification during fruit ripening in tomato (Solanum lycopersicum) PLOS One 8:
- 586 e78949.
- Johnston, S.L., Prakash, R., Chen, N.J., Kumagai, M.H., Turano, H.M., Cooney, J.M.,
- Atkinson, R.G., Paull, R.E., Cheetamun, R., Bacic, A., Brummell, D.A., Schroder, R.
- 589 (2013) An enzyme activity capable of endotransglycosylation of heteroxylan
- polysaccharides is present in plant primary cell walls. Planta 237: 173-187.
- Kaczmarska, A., Pieczywek, P.M., Cybulska J., Zdunek, A. (2022) Structure and
- functionality of rhamnogalacturonan I in the cell wall and in solution: a review.
- 593 Carbohydr. Polym. 278: 118909.
- Keegstra, K., Talmadge, K.W., Bauer, W.D., Albersheim, P. (1973) The structure of
- plant cell walls III. A model of the walls of suspension-cultured sycamore cells based on
- the interconnections of the macromolecular components. Plant Physiol. 51: 188-197.
- Knoch, E., Dilokpimol, A., Geshi, N. (2014) Arabinogalactan proteins: focus on
- carbohydrate active enzymes. Front. Plant Sci. 5: 198.
- Lamport, D.T.A., & Varnai, P. (2013) Periplasmic arabinogalactan glycoproteins act as
- calcium capacitor that regulates plant growth and development. New Phytol. 197: 58-64.
- Leivas, C.L., Iacomini M., Cordeiro L.M.C. (2016) Pectic type II arabinogalactans from
- starfruit (Averrhoa carambola L.). Food Chem. 199: 252-257.
- 603 Lemaire, A., Garzon, C.D., Perrin, A., Habrylo, O., Trezel, P., Bassard, S., Lefebvre, V.,
- Wuytswinkel, O.V., Guillaume, A., Pau-Roblot, C., Pelloux, J. (2020) Three novel
- rhamnogalacturonan I-pectins degrading enzymes from Aspergillus aculeatinus:
- biochemical characterization and application potential. Carbohydr. Polym. 248: 116752.
- Lopez-Hernandez, F., Tryfona, T., Rizza, A., Yu, X.L., Harris, M.O.B., Webb, A.A.R.,
- Kotake, T., Dupree, P. (2020) Calcium binding by arabinogalactan polysaccharides is
- important for normal plant development. Plant Cell 32: 3346-3369.
- 610 Luis, A.S., Briggs, J., Zhang, X., Farnell, B., Ndeh, D., Labourel, A., Basle, A., Cartmell,
- A., Terrapon, N., Scott, K., Lowel, E.C., McLean, R., Shearer, K., Schuckel, J., Venditto,
- 612 I., Ralet, M., Henrissat, B., Martens, E.C., Mosimann, S.C., Abbott, D.W., Gilbert, H.J.

- 613 (2018) Dietary pectic glycans are degraded by coordinated enzyme pathways in human
- 614 colonic Bacteroides. Nat. Microbiol. 3: 210-219.
- Makarova, E.N., & Shakhmatov, E.G. (2021) Characterization of pectin-xylan-glucan-
- arabinogalactan proteins complex from Siberian fir Abies sibirica Ledeb. Carbohydr.
- 617 Polym. 260: 117825.
- McKee, L.S., Rosa, S.L.L., Westereng, B., Eijsink, V.G., Pope P.B., Larsbrink, J. (2021)
- Polysaccharide degradation by the Bacteroidetes: mechanisms and nomenclature.
- 620 Environ. Microbiol. Rep. 13: 559-581.
- McKenna, C., Al-Assaf, S., Phillips, G.O., Funami, T. (2006) The protein component in
- 622 pectin: Is it an AGP? FFI J. 211: 264-274.
- Mohnen, D. (2008) Pectin structure and biosynthesis. Curr. Opin. Plant Biol. 11: 266-
- 624 277.
- Munoz-Munoz, J., Ndeh, D., Fernandez-Julia, P., Walton, G., Henrissat, B., Gilbert, H.J.
- 626 (2021) Sulfation of arabinogalactan proteins confers privileged nutrient status to
- Bacteroides plebeius. mBio 12: e01368-21.
- Mutter, M., Colquhoun, I.J., Beldman, G., Schols, H.A., Bakx, E.J., Voragen, A.G.J.
- 629 (1998) Characterization of recombinant rhamnogalacturonan α-L-rhamnopyranosyl-1-
- 630 (1,4)-α-D-galactopyranosyluronide lyase from *Aspergillus aculeatus*. Plant Physiol. 117:
- 631 141-152.
- Nascimento, G.E.d., Iacomini, M., Cordeiro, L.M.C. (2017) New findings on green sweet
- pepper (Capsicum annum) pectins: rhamnogalacturonan and type I and II
- arabinogalactans. Carbohydr. Polym. 171: 292-299.
- Ndeh, D., & Gilbert, H.J. (2018) Biochemistry of complex glycan depolymerization by
- the human gut microbiota. FEMS Microbiol. Rev. 42: 146-164.
- Ndeh, D., Rogowski, A., Cartmell, A., Luis, A.S., Basle, A., Gray, J., Venditto, I.,
- Briggs, J., Zhang, X., Labourel, A., Terrapon, N., Buffetto, F., Nepogodiev, S., Xiao, Y.,
- 639 Field, R.A., Zhu, Y., O'Neill, M.A., Urbanowicz, B.R., York, W.S., Davies, G.J., Abbott,
- D.W., Ralet, M.C., Martens, E.C., Henrissat, B., Gilbert, H.J. (2017) Complex pectin
- 641 metabolism by gut bacteria reveals novel catalytic functions. Nature 544: 65-70.

- Ndukwe, I.E., Black, I., Heiss, C., Azadi P. (2020) Evaluating the utility of permethylated
- polysaccharide solution NMR data for characterization of insoluble plant cell wall
- 644 polysaccharides. Anal. Chem. 92: 13221-13228
- Nergard, C.S., Matsumoto, T., Inngjerdingen, M., Inngjerdingen, K., Hokputsa, S.,
- Harding, S.E., Michaelsen, T.E., Diallo, D., Kiyohara, H., Paulsen, B.S., Yamada, H.
- 647 (2005) Structural and immunological studies of a pectin and a pectic arabinogalactan
- 648 from Vernonia kotschyana Sch. Bip. Ex Walp. (Asteraceae). Carbohydr. Res. 340: 115-
- 649 130.
- Oosterveld, A., Voragen, A.G.J., Schols, H.A. (2002) Characterization of hop pectins
- shows the presence of an arabinogalactan-protein. Carbohydr. Polym. 49: 407-413.
- Pellerin, P., Vidal, S., Williams, P., Brillouet, J.M. (1995) Characterization of five type II
- arabinogalactan-protein fractions from red wine of increasing uronic acid content.
- 654 Carbohydr. Res. 277: 135-143.
- Pfeifer, L., Shafee, T., Johnson, K., Bacic, A., Classen, B. (2020) Arabinogalactan-
- 656 proteins of Zostera marina L. contain unique glycan structures and provide insight into
- adaption processes to saline environments. Sci. Rep. 10: 8232.
- Phillips, L.R., & Fraser, B.A. (1981) Methylation of carbohydrates with dimsyl
- potassium in dimethyl sulfoxide. Carbohydr. Res. 90: 149-152.
- Ropartz, D., & Ralet, M.-C. (2020) Pectin structure. In V. Kontogiorgos (Ed.) *Pectin:*
- 661 *Technological and physiological properties* (pp. 17-36). Switzerland: Springer Nature.
- Ryden, P., & Selvendran, R.R. (1990) Cell-wall polysaccharides and glycoproteins of
- parenchymatous tissues of runner bean (Phaseolus coccineus). Biochem. J. 269: 393-402.
- Santander, J., Martin, T., Loh, A., Pohlenz, C., Gatlin III, D.M., Curtiss III, R. (2013)
- Mechanisms of intrinsic resistance to antimicrobial peptides of Edwardsiella ictaluri and
- its influence on fish gut inflammation and virulence. Microbiology 159: 1471-1486.
- 667 Saulnier, L., & Brillouet, J.M. (1988) Structural studies of pectic substances from the
- 668 pulp of grape berries. 182: 63-78.
- 669 Shimoda, R., Okabe, K., Kotake, T., Matsuoka, K., Koyama, T., Tryfona, T., Liang,
- H.C., Dupree, P., Tsumuraya, Y. (2014) Enzymatic fragmentation of carbohydrate
- 671 moieties of radish arabinogalactan-protein and eluciation of the structures. Biosci.
- 672 Biotechnol. Biochem. 78: 818-831.

- 673 Sun, Y., Cui, S.W., Tang, J., Gu, X. (2010) Structural features of pectic polysaccharide
- 674 from *Angelica sinensis* (Oliv.) Diels. Carbohydr. Polym. 80: 544-550.
- 675 Tan, L., Leykam, J.F., Kieliszewski, M.J. (2003) Glycosylation motifs that direct
- arabinogalactan addition to arabinogalactan-proteins. Plant Physiol. 132: 1362-1369.
- 677 Tan, L., Qiu, F., Lamport, D.T.A., Kieliszewski, M.J. (2004) Structure of a
- 678 hydroxyproline (Hyp)-arabinogalactan polysaccharide from repetitive Ala-Hyp expressed
- in transgenic *Nicotiana tabacum*. J. Bio. Chem. 279: 13156-13165.
- 680 Tan, L., Varnai, P., Lamport, D.T.A., Yuan, C., Xu, J., Qiu, F., Kieliszewski, M.J. (2010)
- Plant O-hydroxyproline arabinogalactans are composed of repeating trigalactosyl
- subunits with short bifurcated side chains. J. Biol. Chem. 285: 24575-24583.
- Tan, L., Showalter, A.M., Egelund, J., Hernandez-Sanchez, A., Doblin, M.S., Bacic, A.
- 684 (2012) Arabinogalactan-proteins and the research challenges for these enigmatic plant
- cell surface proteoglycans. Front. Plant Sci. 3: 140.
- Tan, L., Eberhard, S., Pattathil, S., Warder, C., Glushka, J., Yuan, C., Hao, Z., Zhu, X.,
- Avci, U., Miller, J.S., Baldwin, D., Pham, C., Orlando, R., Darvill, A., Hahn, M.G.,
- Kieliszewski, M.J., Mohnen, D. (2013) An Arabidopsis cell wall proteoglycan consists of
- pectin and arabinoxylan covalently linked to an arabinogalactan protein. Plant Cell 25:
- 690 270-287.
- Tryfona, T., Liang, H.C., Kotake, T., Kaneko, S., Marsh, J., Ichinose, H., Lovegrove, A.,
- Tsumuraya, Y., Shewry, P.R., Stephens, E., Dupree, P. (2010) Carbohydrate structural
- analysis of wheat flour arabinogalactan protein. Carbohydr. Res. 345: 2648-2656.
- Tryfona, T., Liang, H.C., Kotake, T., Tsumuraya, Y., Stephens, E., Dupree, P. (2012)
- 695 Structural characterization of Arabidopsis leaf arabinogalactan polysaccharides. Plant
- 696 Physiol. 160: 653-666.
- Tsumuraya, Y., Mochizuki, N., Hashimoto, Y., Kovac, P. (1990) Purification of an exo-
- 698  $\beta$ -(1,3)-D-galactanase of Irpex lacteus (Polyporus tulipiferae) and its action on
- arabinogalctan-proteins. J. Biol. Chem. 265: 7207-7215.
- Voragen, A.G.J., Coenen, G.-J., Verhoef, R.P., Schols, H.A. (2009) Pectin, a versatile
- 701 polysaccharide present in plant cell walls. Struct. Chem. 20: 263.
- Willis, L.M., Stupak, J., Richards, M.R., Lowary, T.L., Li, J., Whitfield, C. (2013)
- 703 Conserved glycolipid termini in capsular polysaccharides synthesized by ATP-binding

- cassette transporter-dependent pathways in Gram-negative pathogens. Proc. Natl. Acad.
- 705 Sci. U.S.A. 110: 7868-7873.
- Yamada, H., Yanahira, S., Kiyohara, H., Cyong, J.C., Otsuka, Y. (1987) Characterization
- of anti-complimentary acidic heteroglycans from the seeds of Coix lacryma-jobivar Ma-
- 708 yuen. Phytochemistry 26: 3269-3275.
- York, W.S., Darvill, A.G., McNeil, M., Stevenson, T.T., Albersheim, P. (1986) Isolation
- and characterization of plant cell walls and cell wall components. Methods Enzymol.
- 711 118: 3-40.
- 712 Zheng, Y., & Mort, A. (2008) Isolation and structural characterization of a novel
- oligosaccharide from the rhamonogalacturonan of *Gossypium hirsutum* L. Carbohydr.
- 714 Res. 343: 1041-1049.